netic hole centers are completely annealed. This is checked by cooling the sample to 80°K and looking by means of EPR for the hole spectrum.

Our high-resolution thermoluminescence spectra of Gd^{3+} in SrF_2 and BaF_2 show that both cubic and axial symmetry rare-earth ions are converted to the divalent state. In CaF_2 it has been shown that after irradiation only cubic-symmetry divalent ions are found.[6,19,20] In BaF_2, however, Tm^{2+} is found in trigonal and cubic symmetry, and the possibility of switching from one symmetry to another by light illumination has been demonstrated.[21] At lowest temperatures, the recombination of hole and Re^{2+} occurs in the axial symmetry site. The pair Re^{2+}-F^- attracts a hole. In higher temperatures, the cubic converted sites recombine.

A more detailed study of the V_K' is needed in order to establish the trapping mechanism by a local negative charge more precisely. Electron-nuclear double-resonance measurements probably are needed. The details of the self-trapping process could be revealed also by this technique.

The complexity of the centers in CaF_2 does not allow us to understand the nature of the six glow peaks[2] found there.

In conclusion, we would like to point out that we found two new centers in SrF_2 and BaF_2, namely, V_H and V_K' centers. The nature of the V_H centers is well established in this work. An experimentally verified model is given to explain the existence of various thermoluminescent glow peaks.

[19] W. Hayes, G. D. Jones, and J. W. Twidell, Proc. Phys. Soc. (London) **81**, 371 (1963).
[20] W. Hayes and J. W. Twidell, Proc. Phys. Soc. (London) **82**, 330 (1963).
[21] E. S. Sabisky and C. H. Anderson, Phys. Rev. **159**, 234 (1967).

PHYSICAL REVIEW VOLUME 182, NUMBER 3 15 JUNE 1969

Optical Phonons and Symmetry of Tysonite Lanthanide Fluorides

R. P. LOWNDES,* J. F. PARRISH, AND C. H. PERRY*
Spectroscopy Laboratory† and Research Laboratory of Electronics,‡ Massachusetts Institute of Technology, Cambridge, Massachusetts 02139
(Received 19 December 1968)

The polarized infrared reflectance of LaF_3, CeF_3, PrF_3, and NdF_3 has been measured from 40 to 500 cm^{-1} at 295, 78, and 7°K. Kramers-Kronig analyses of the reflectance spectra yield evidence for eleven infrared-active phonons in the σ polarization ($\mathbf{E}\perp c$) and six in the π polarization ($\mathbf{E}\|c$). These results, together with reported magnetic-resonance measurements, are consistent with a $P\bar{3}'c'1$ magnetic space group. A theory and method for directly observing the longitudinal optical phonon frequencies of strongly anisotropic crystals in transmission are reported.

INTRODUCTION

THE partially filled $4f$ electron shell of the lanthanide elements is so well screened from its external environment that, when the ions are held in a suitable host lattice, electronic transitions of the type $4f \rightarrow 4f$ are expected to give sharp spectral lines. Some of the known $4f \rightarrow 4f$ transitions lie in the far-infrared region of the spectrum.[1–5] Consequently, there is currently strong motivation to assess the potential of these low-energy transitions for use in solid-state far-infrared lasers.

It is clear, however, that in order to investigate these potential far-infrared lasing systems, the host lattice must be chosen with care. This is true not only because the host lattice will determine the position and linewidth of the $4f \rightarrow 4f$ transitions, but also because the optically active phonon frequencies of most solids lie within the far-infrared region as well, and precautions should be taken to ensure that the frequencies of the electronic and phonon excitations do not significantly overlap.

The tysonite structure of LaF_3, CeF_3, PrF_3, and NdF_3 provides a convenient host lattice in which other lanthanide ions will enter substitutionally. These substances are rugged[6,7] and readily available in single-crystal form.[8] Their nonhygroscopic nature[6,7] has the spectroscopic advantage that they are unlikely to incorporate OH^- impurities which are well known to

* Present address: Department of Physics, Northeastern University, Boston, Mass. 02115.
† Laboratory supported in part by National Science Foundation Grant No. GP-4923.
‡ Work supported in part by the Joint Services Electronics Program [Contract No. DA 28-043-AMC 02536 (E)], by NASA [Grant No. NGR 22-009-(237)], and by the U. S. Air Force [ESD Contract No. AF 19(628)-6066].
[1] S. A. Johnson, H. G. Freie, A. L. Schawlow, and W. M. Yen, J. Opt. Soc. Am. **57**, 734 (1967).
[2] R. A. Buchanan, H. E. Rast, and H. H. Caspers, J. Chem. Phys. **44**, 4063 (1966).
[3] W. F. Krupke and J. B. Gruber, J. Chem. Phys. **39**, 1024 (1963).
[4] E. V. Sayre and S. Freed, J. Chem. Phys. **23**, 2066 (1955).
[5] R. P. Bauman and S. P. S. Porto, Phys. Rev. **161**, 842 (1967).
[6] J. B. Mooney, Infrared Phys. **6**, 153 (1966).
[7] G. Hass, J. B. Ramsey, and R. Thun, J. Opt. Soc. Am. **49**, 116 (1959).
[8] Optovac, Inc., North Brookfield, Mass.

contribute defect modes to the phonon spectrum of a host lattice.[9]

X-ray–diffraction studies have led to three commonly proposed lattices for the tysonite structure: a hexamolecular cell with $P6_3/mcm$ (D_{6h}^3) symmetry,[10,11] a bimolecular cell with $P6_3/mmc$ (D_{6h}^4) symmetry,[12] and a hexamolecular cell with $P\bar{3}c1$ (D_{3d}^4) symmetry.[13–15] Faraday or paramagnetic rotation,[16,17] electron-spin resonance,[18–20] and optical absorption measurements[1–4,21–28] have provided a substantial amount of additional experimental evidence but the proper space group for the tysonite structure has not yet been conclusively established. In fact, some of the magnetic-resonance data[18,19] appear inconsistent with all three of the above lattices. Recently, Baumann and Porto[5] reported the frequencies and polarizations of the Raman-active phonon modes for these four tysonite lanthanide fluorides. For LaF_3 at least, their results strongly favor the hexamolecular $P\bar{3}c1$ lattice.

The frequencies and polarizations of the fundamental infrared-active phonon modes are, for the most part, not known for these compounds, although some attempts have been made to determine them for LaF_3 from transmission measurements on polycrystalline samples[29] and from unpolarized emittance spectra.[30] However, since the lanthanide fluorides are uniaxial, the dielectric response tensor contains two principal nondegenerate components, and the infrared-active modes can only be measured uniquely by using radiation polarized separately along these two orthogonal components. Consequently, these previous experiments have not necessarily identified all of the fundamental phonon transitions.

This paper complements the recent Raman study[5] and reports a complete set of polarized, fundamental, infrared-active phonon modes for LaF_3, CeF_3, PrF_3, and NdF_3 at temperatures between 7 and 295°K. These infrared results for the tysonite lattice, together with the Raman results, are consistent only with the $P\bar{3}c1$ (D_{3d}^4) lattice containing six formula units per unit cell and conclusively eliminate the $P6_3/mcm$ and $P6_3/mmc$ lattices. In order to be consistent with the magnetic-resonance data, the proper magnetic space group must be $P\bar{3}'c'1$.

EXPERIMENTAL DETAILS

Cylindrical single crystals of LaF_3, CeF_3, PrF_3, and NdF_3 10 mm in diam and approximately 5 mm long were obtained from Optovac, Inc.[8] The crystals were supplied with the c axis perpendicular to the cylinder axis and parallel to the plane of the circular end faces. Using crossed polarizers, the c axis could be oriented with respect to the polarization of the incident radiation to better than 5°, which resulted in an intermixing between the orthogonal polarizations of less than 2% reflectance. Only the CeF_3 sample showed the hexagonal striations reported to be associated with oxygen impurities.[6]

The reflectance and transmittance spectra were measured with an R.I.I.C. FS-520 Fourier spectrometer (Michelson type) adapted for 12-bit analog-to-digital conversion. A mercury arc source in conjunction with a liquid-helium–cooled Ga-doped germanium bolometer was used from 40 to 200 cm^{-1}. A Nernst glower with a Golay pneumatic cell was used from 150 to 650 cm^{-1}. A vacuum-evaporated one-dimensional wire-grid polarizer was used to reduce the horizontally polarized radiation to much less than 1% of the vertically polarized component.[31]

The normalized transmittance was calculated using an aperture the same size as the sample. The normalized reflectance was calculated using an aluminum mirror as a reference background. The plane of incidence was horizontal and the angle of incidence was approximately $7\frac{1}{2}°$. By orienting the crystal so that the c axis lay in the face of the crystal and was either vertical or horizontal, either the π component ($E\|c$) or the σ component ($E\perp c$) of the dielectric response tensor could be individually excited.

DIELECTRIC RESPONSE TENSOR

The effective dielectric response function for each tensor component was calculated from a Kramers-Kronig analysis of the reflectance measurements using the Fresnel formula appropriate for a crystal aligned with the desired axis precisely parallel to the incident electric field and perpendicular to the plane of incidence. The infrared-active transverse optical (TO) frequencies

[9] D. R. Bosomworth, Solid State Commun. **5**, 681 (1967).
[10] I. Oftedal, Z. Physik. Chem. **5B**, 272 (1929).
[11] I. Oftedal, Z. Physik. Chem. **13B**, 190 (1931).
[12] K. Schlyter, Arkiv Kemi **5**, 73 (1953).
[13] M. Mansmann, Z. Anorg. Allgem. Chem. **331**, 98 (1964).
[14] M. Mansmann, Z. Krist. **122**, 375 (1965).
[15] A. Zalkin, D. H. Templeton, and T. E. Hopkins, Inorg. Chem. **5**, 1466 (1966).
[16] J. H. Van Vleck and M. H. Hebb, Phys. Rev. **46**, 17 (1934).
[17] J. Becquerel, W. J. de Haas, and J. Van den Handel, Physica **1**, 383 (1934).
[18] M. B. Schulz and C. D. Jeffries, Phys. Rev. **149**, 270 (1966).
[19] J. M. Baker and R. S. Rubins, Proc. Phys. Soc. (London) **78**, 1353 (1961).
[20] D. A. Jones, J. M. Baker, and D. F. D. Pope, Proc. Phys. Soc. (London) **74**, 249 (1959).
[21] A. Hadni and P. Strimer, Compt. Rend. **265**, B811 (1967).
[22] G. D. Jones and R. A. Satten, Phys. Rev. **147**, 566 (1966).
[23] H. H. Caspers, H. E. Rast, and R. A. Buchanan, J. Chem. Phys. **42**, 3214 (1965).
[24] H. H. Caspers, H. E. Rast, and R. A. Buchanan, J. Chem. Phys. **43**, 2124 (1965).
[25] W. M. Yen, W. C. Scott, and A. L. Schawlow, Phys. Rev. **136**, A271 (1964).
[26] A. Hadni, X. Gerbaux, G. Morlot, and P. Strimer, J. Appl. Phys. (Japan) **4**, 574 (1965).
[27] E. Y. Wong, O. M. Stafsudd, and D. R. Johnston, J. Chem. Phys. **39**, 786 (1963).
[28] E. Y. Wong, O. M. Stafsudd, and D. R. Johnston, Phys. Rev. **131**, 990 (1963).
[29] H. H. Caspers, R. A. Buchanan, and H. R. Marlin, J. Chem. Phys. **41**, 94 (1964).
[30] H. E. Rast, H. H. Caspers, S. A. Miller, and R. A. Buchanan, Phys. Rev. **171**, 1051 (1968).
[31] C. H. Perry, R. Geick, and E. F. Young, Appl. Opt. **5**, 1171 (1966).

associated with the poles of the dielectric response function ($|D|\neq 0$, $|E|\to 0$) were located by peaks in $\omega\epsilon''$ ($\hat{\epsilon}=\epsilon'+i\epsilon''$), which is proportional to the electric conductivity $\sigma=\omega\epsilon''/4\pi$. The infrared-active longitudinal optical (LO) frequencies associated with the zeros of the dielectric response function ($|D|\to 0$, $|E|\neq 0$)[32,33] were located by peaks in $-\omega\eta''$ ($\hat{\epsilon}^{-1}=\hat{\eta}=\eta'+i\eta''$, $\eta''=-\epsilon''/|\hat{\epsilon}|$).

The principal poles and zeros of the two components of the dielectric response tensor were identified quite satisfactorily using the above procedure. However, there were measurable effects in both reflectance and transmittance due to a slight misalignment of the crystal axes. In order to understand the nature and magnitude of the effects of this misalignment, it is instructive to solve a special case of the reflectance and transmittance of a uniaxial crystal.

In a uniaxial crystal ($\epsilon_x=\epsilon_y\neq\epsilon_z$), the incident radiation splits into an ordinary wave and an extraordinary wave which propagate independently of one another. If the direction of propagation of the incident radiation is normal to the crystal-vacuum interface, the ordinary and extraordinary waves propagate in the same direction as the incident radiation. If φ is the angle between the incident electric field and the projection of the c axis on the crystal face, it can be easily shown that $R=R_0\sin^2\varphi+R_e\cos^2\varphi$ and $T=T_0\sin^2\varphi+T_e\cos^2\varphi$, where R and T are the effective normal reflectance and transmittance coefficients of the crystal, and R_0, T_0, R_e, and T_e are the normal reflectance and transmittance coefficients for the ordinary wave and the extraordinary wave, respectively.

If $\varphi\approx 0$, then $R=R_e+(R_0-R_e)\sin^2\varphi\approx R_e$. Since $|R_0-R_e|\leq 1$ and in practice $\sin^2\varphi\leq 0.01$, it is clear that one can measure the extraordinary reflectance coefficient within an additive error of less than 1% reflectance. Similarly, if $\varphi\approx 90°$, the ordinary reflectance coefficient can be measured within 1% reflectance. As a result, the errors introduced in the measurement of the reflectance or transmittance by a slight error ($<5°$) in the orientation of the plane of polarization with respect to the optical axis can either be conveniently ignored or be eliminated by small corrections based upon measurements in the orthogonal plane of polarization.

Moreover, since $R_0=|(1-\hat{n}_x)/(1+\hat{n}_x)|^2$ and, ignoring interference effects, $T_0\approx(1-R_0)^2e^{-\alpha_x d}$, where $\hat{n}_x=(\mu\epsilon_x)^{1/2}$, $d\equiv$thickness of the crystal, and $\alpha_x=2\pi\omega\,\mathrm{Im}(\hat{n}_x)$, one of the components of the dielectric response tensor ϵ_x can be calculated directly from R_0 and T_0.

Unfortunately, ϵ_z can not be calculated directly from R_e and T_e. $R_e=|(1-\hat{n}_e)/(1+\hat{n}_e)|^2$ and, ignoring interference effects, $T_e\approx(1-R_e)^2e^{-\alpha_e d}$, where $\hat{n}_e=c/v_e$ and $\alpha_e=2\pi\omega\,\mathrm{Im}(\hat{n}_e)$, but $v_e^2=v_z^2\cos^2\theta+v_x^2\sin^2\theta$, where $v_x^2=c^2/\mu\hat{\epsilon}_x$, $v_z^2=c^2/\mu\hat{\epsilon}_z$, and θ is the angle between the c axis and the plane of the crystal face.

The crystals used in this study were cut and polished with the c axis parallel to the face of the crystal within an estimated 5°, so that $\sin^2\theta\approx\theta^2\leq 0.01$ and $v_e^2\approx v_z^2+(v_x^2-v_z^2)\theta^2$. Equivalently,

$$\hat{n}_e\approx\hat{n}_z[1+\theta^2(\epsilon_z/\epsilon_x-1)]^{-1/2}\approx\hat{n}_z-(\theta^2/2\epsilon_x)\hat{n}_z(\epsilon_z-\epsilon_x)$$

as long as $|\theta^2/\epsilon_x|\ll 1$. Under these conditions,

$$R_e\approx R_z\pm 2\theta^2R_z\left|\frac{\hat{n}_z}{1-\epsilon_z}\right|\cdot\left|\frac{\epsilon_z-\epsilon_x}{\epsilon_x}\right|$$

and $T_e\approx(1-R_e)^2e^{-\alpha_e d}$, where $R_z=|(1-\hat{n}_z)/(1+\hat{n}_z)|^2$, $\alpha_e\approx\alpha_z-\pi\omega\,\mathrm{Im}[(\theta^2/\epsilon_x)\hat{n}_z(\epsilon_z-\epsilon_x)]$, $\hat{n}_z=(\mu\epsilon_z)^{1/2}$, and $\alpha_z=2\pi\omega\,\mathrm{Im}(\hat{n}_z)$.

Clearly, even when $\theta^2\leq 0.01$, there is no assurance that the difference between R_e and R_z and between T_e and T_z must be less than 1%. In fact, whenever $|\epsilon_x|\to 0$, that is, whenever one is near a pole of $\eta_x=\epsilon_x^{-1}$, significant features may be expected in R_e and T_e. In a low-dispersion region of ϵ_z in which $\mathrm{Re}(\hat{n}_z)\approx\mathrm{const}=n_z$ and $\mathrm{Im}(\hat{n}_z)\to 0$, then $R_e\approx R_z+K_1\theta^2/|\epsilon_x|$ and $\alpha_e\approx -K_2\theta^2\omega\eta_x''$, where $\eta_x''=\mathrm{Im}(\epsilon_x^{-1})$ and $K_2=\pi n_z^3/\mu$, and where K_1 may be evaluated from R_e and R_0. Consequently, even in regions where ϵ_z is approximately constant, there will be a weak peak in the reflectance and a moderately strong minimum in the transmittance proportional to θ^2 whenever the frequency approaches a LO frequency of ϵ_x. Minima in the extraordinary transmittance near poles of $\hat{\eta}_z=\hat{\epsilon}_z^{-1}$ due to the LO frequencies of ϵ_z can be observed as well for radiation propagating almost parallel to the optical axis.

This weak coupling of the nominally transverse material electromagnetic wave (mixed photon-phonon particle wave) to the LO frequencies of the orthogonal components of the dielectric response tensor apparently has not been previously reported although it is a general property of all strongly anisotropic ($|\hat{\epsilon}_x-\hat{\epsilon}_z|\gg 0$) transparent crystals. The existence of this effect makes it possible for some longitudinal dielectric resonances to be studied in transmission, as if they were weak transverse resonances, as well as identifying intrinsic but otherwise spurious absorption bands due to a slight misalignment of an anisotropic crystal with strong longitudinal resonances.

An observation of the lowest LO frequency of the $\hat{\epsilon}_x$ component of the tysonite lanthanide fluorides is reported in the next section.

EXPERIMENTAL RESULTS

Figure 1 shows the measured specular reflectance of LaF_3, CeF_3, PrF_3, and NdF_3 at 7°K with $E\|c$ (π-polarized modes). Five infrared-active phonon modes are clearly visible in all four materials. An additional band is observed at 234 cm^{-1} for PrF_3 and at 239 cm^{-1} for NdF_3 which may be a sixth fundamental phonon

[32] A. S. Barker, Jr., in *Ferroelectricity*, edited by Edward F. Weller (Elsevier Publishing Co., Amsterdam, 1967), pp. 219–250.
[33] D. W. Berreman and F. C. Unterwald, Phys. Rev. 174, 791 (1968).

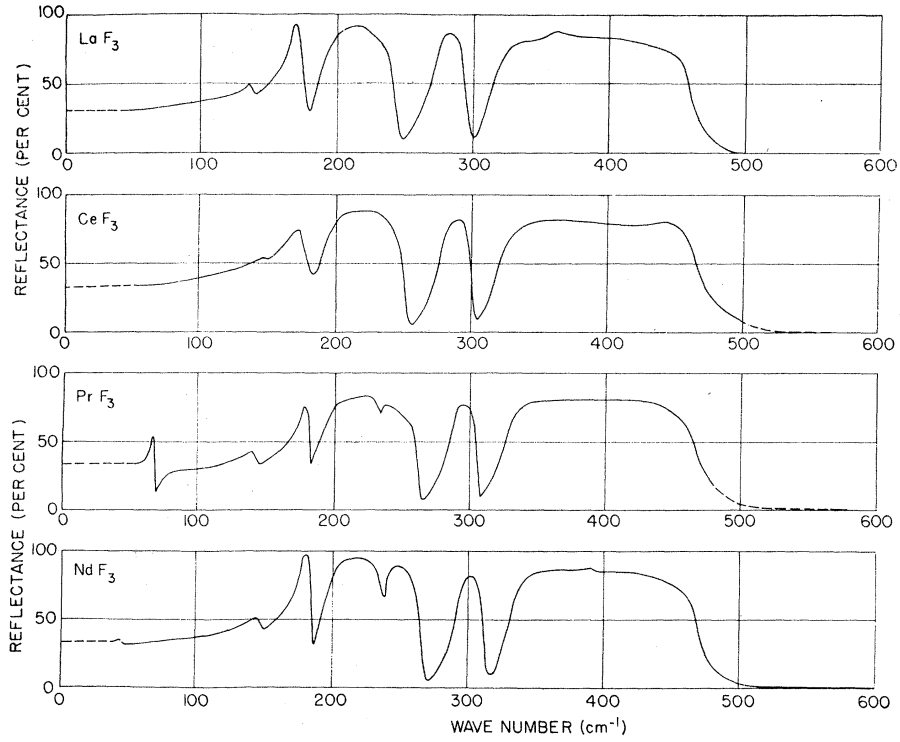

FIG. 1. Far-infrared reflectance of the lanthanide fluorides at 7°K in the π polarization.

mode due to the lifting of an accidental degeneracy. For PrF_3, an additional band at 66 cm^{-1} is also observed which is not present in the reflectance spectra of the other salts. This band is believed to be due to an electronic transition from the ground state to the first excited state of the $^3H_4$ Stark multiplet of Pr^{3+}. This transition has been predicted from optical absorption measurements[4,21,24–27] to occur near 66 cm^{-1} and its nature has been confirmed on the basis of far-infrared transmission measurements of Pr^{3+} contained within

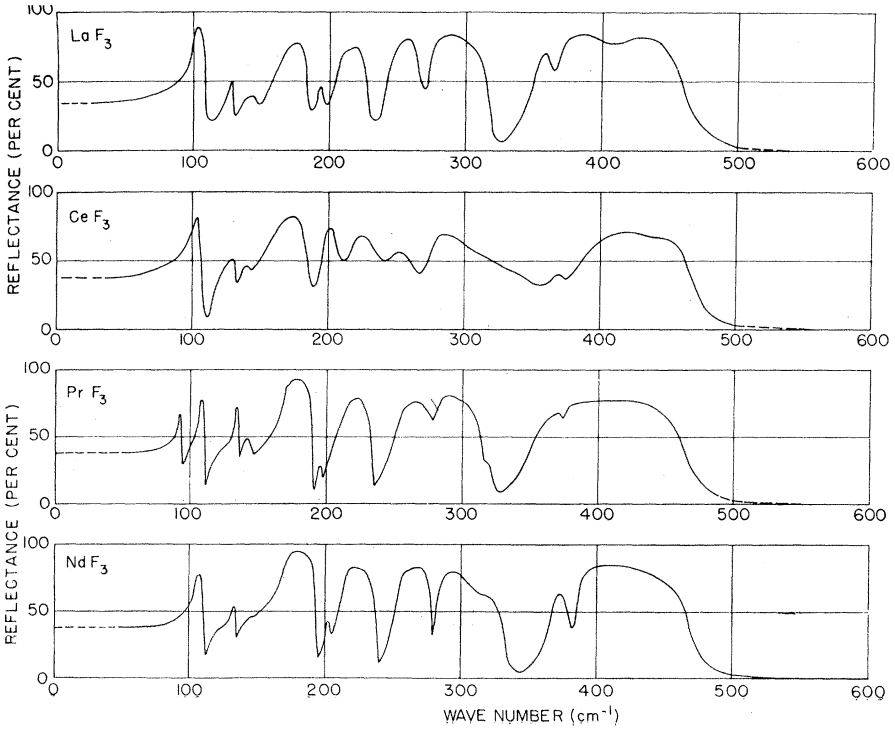

FIG. 2. Far-infrared reflectance of the lanthanide fluorides at 7°K in the σ polarization.

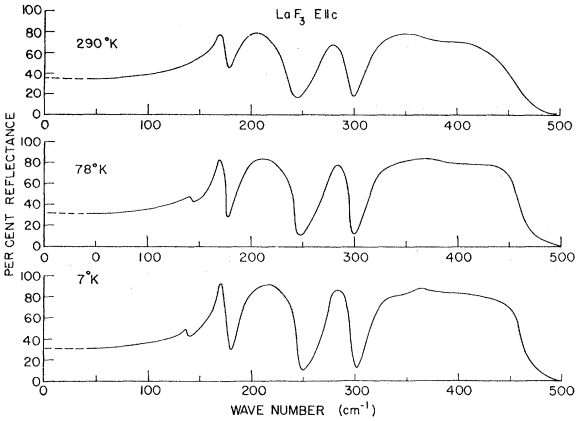

FIG. 3. Temperature dependence of the far-infrared reflectance of LaF_3 in the π polarization.

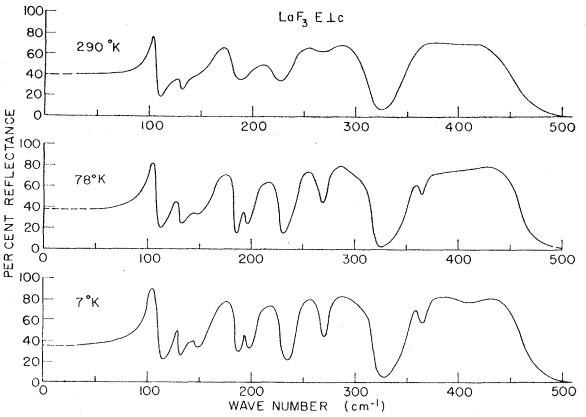

FIG. 4. Temperature dependence of the far-infrared reflectance of LaF_3 in the σ polarization.

these four host lattices.[34] A perceptible change in the reflectance of NdF_3 was also observed in this polarization near 45 cm^{-1} due to an electronic transition from the ground state to the first excited state of the $^4I_{9/2}$ Stark multiplet of the Nd^{3+} ion. This latter transition has been confirmed to be electronic in nature by Zeeman splitting.[34]

Figure 2 shows the measured specular reflectance for the four salts at 7°K with $E \perp c$ (σ-polarized modes). In this polarization at least ten well-defined infrared-active phonon modes are observed, although the reflection band centered near 140 cm^{-1} in LaF_3 is only partially resolved in NdF_3. Proceeding through the series from LaF_3 through NdF_3, a moderately strong shoulder appears on the low-frequency side of the reflection band near 130 cm^{-1} (in LaF_3) and it is quite likely that there are in fact eleven infrared-active phonon modes in the σ polarization. For PrF_3, an additional reflection band (at 92 cm^{-1}) is once again observed which is not present in the spectra of the other salts. This mode is believed

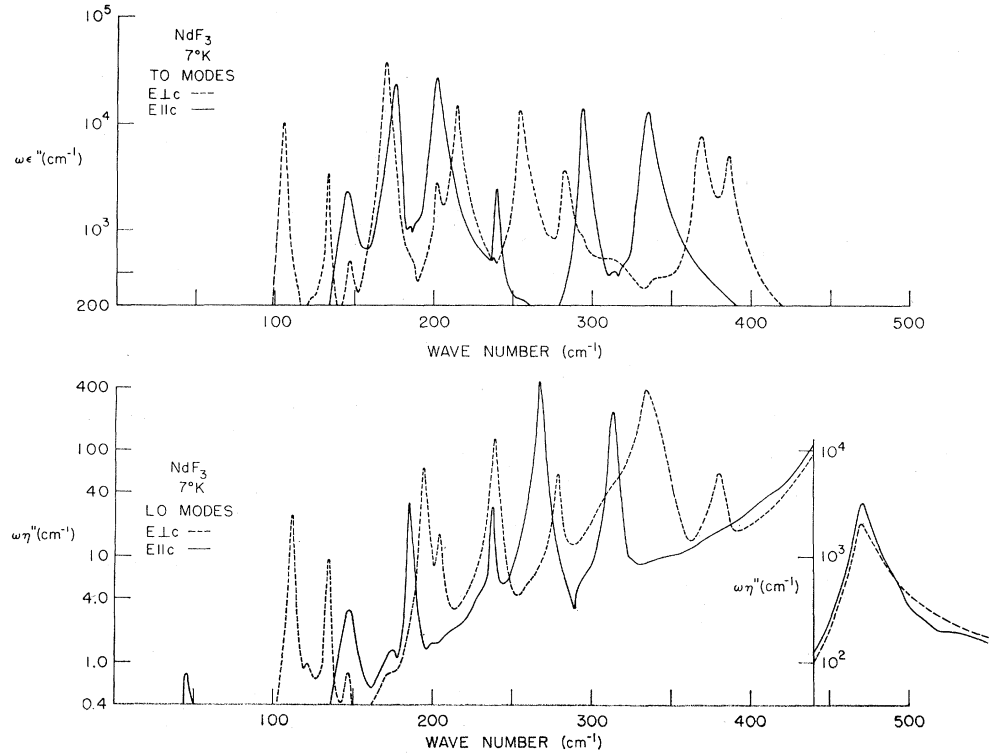

FIG. 5. Frequency dependence of the dielectric functions $\omega\epsilon''$ and $\omega\eta''$ for NdF_3 at 7°K.

[34] J. F. Parrish, Ph.D. thesis, Department of Physics, MIT, 1969 (unpublished).

TABLE I. Transverse and longitudinal $k\approx 0$ phonon frequencies and their associated damping in cm^{-1} for the lanthanide fluorides in the π polarization. The phonon frequencies are accurate to ± 2 cm^{-1} and the damping to $\pm 20\%$.

	LaF_3			CeF_3			PrF_3			NdF_3		
°K	5	78	295	5	78	295	5	78	295	5	78	295
ω_T	138	142		140	141		141	141		144	147	
γ_T	3	5		9	9		5	16		10		
ω_L	138	143		140	141		143	142		147	147	
γ_L	4	5		8	8		5	17		10		
ω_T	166	168	168	170	170	167	178	175	170	176	177	172
γ_T	4	4	6	5	6	10	3	9	16	5	4	8
ω_L	178	178	176	180	181	180	183	182	182	185	185	184
γ_L	3	4	7	6	10	20	2	6	15	3	3	12
ω_T	194	195	194	199	203	193	201	203	195	202	202	198
γ_T	8	9	14	8	11	24	10	17	20	6	7	15
ω_L	246	243	239	252	252	249	263	261	257	268	267	264
γ_L	5	7	16	8	8	16	6	7	20	4	6	14
ω_T							234	232		240	238	236
γ_T										3	6	
ω_L							234	232		238	236	234
γ_L										4	5	
ω_T	273	274	275	280	285	273	289	288	283	294	294	290
γ_T	8	10	12	3	6	20	6	8	20	4	6	17
ω_L	298	297	296	302	301	303	308	307	308	314	314	312
γ_L	6	6	10	4	7	13	5	4	20	5	6	14
ω_T	318	319	323	329	339	321	331	332	339	335	337	337
γ_T	14	14	16	6	14	18	8	15	20	8	8	12
ω_L	462	461	468	478	475	466	471	474	467	470	472	472
γ_L	14	18	62	23	38	17	15	20	20	13	18	44

to be due to an electronic transition from the ground state of the $^3H_4$ Stark multiplet of the Pr^{3+} ion to the second excited state for the same reasons as given above for the electronic transitions observed in the π polarization.

Figures 3 and 4 illustrate, respectively, the temperature dependence typical of the reflectance spectra in the π and σ polarizations for LaF_3 between 7 and 295°K. It is evident that a fairly rapid damping of the weaker reflection bands occurs as the temperature is raised, so that at 295°K there are only four well-defined reflection bands in the π polarization and seven in the σ polarization. The damping out of the weaker reflection bands is a continuous process with increasing temperature and there is no evidence for a phase change.

Kramers-Kronig analyses of the reflectance measurements determined the dielectric functions $\omega\epsilon''$ and $\omega\eta''$ for each lanthanide fluoride. Figure 5 shows the typical shape of these functions for NdF_3. Six TO and LO frequencies can be easily distinguished in the π polarization, but only ten TO and LO frequencies can be easily seen in the σ polarization. A weak but sharp feature near 125 cm^{-1} in both $\omega\epsilon''$ and $\omega\eta''$ has been interpreted as an eleventh fundamental phonon mode due to its appearance as a shoulder on the low-frequency side of another fundamental phonon mode and because it occurs at a frequency lower than expected for two-phonon summation processes. The weak broad feature near 320 cm^{-1}, which is even weaker than the mode near 125 cm^{-1}, has been interpreted as a two-phonon summation process because it is at a sufficiently high frequency and appears on the high-frequency side of a fundamental phonon mode. Tables I and II summarize the $k\approx 0$ infrared-active TO and LO phonon frequencies and their associated half-widths determined for each of the four lanthanide fluorides from the dielectric functions as described in a preceding section. The tables reveal that the frequency of any particular lattice mode in LaF_3 moves to higher frequencies as the reduced mass of the host lattice is increased. This reflects the stronger interionic forces present in the heavier lattices due to the lanthanide contraction of the cell volume as the atomic number of the cation is increased.[35]

Figure 6 shows the frequency dependence of the absorption coefficient from 40 to 150 cm^{-1} for one sample of LaF_3 at 7°K in both orthogonal polarizations. In the σ polarization, a strong band centered near 103 cm^{-1} dominates the spectrum as predicted by the reflectance measurements. In the π polarization, the weak band centered at 107.7 cm^{-1} with a half-width of approximately 2 cm^{-1} is interpreted as the $k\approx 0$ LO phonon frequency forecast from the reflectance measurements to be between 109 and 110 cm^{-1} with a half-width of approximately 3 cm^{-1}. As explained previously, this weak absorption due to the longitudinal mode varies in strength from sample to sample and is seen because the crystal c axis was slightly misaligned from the $E\|c$ and $k\perp c$ requirements for the π polarization. The ratio of

[35] A. Zalkin and D. H. Templeton, J. Am. Chem. Soc. **75**, 2453 (1953).

TABLE II. Transverse and longitudinal $k\approx 0$ phonon frequencies and their associated damping in cm^{-1} for the lanthanide fluorides in the σ polarization. The phonon frequencies are accurate to ± 2 cm^{-1} and the damping to $\pm 20\%$.

	LaF_3			CeF_3			PrF_3			NdF_3		
°K	5	78	295	5	78	295	5	78	295	5	78	295
ω_T	101	100	100	98	98	100	107	104	102	104	105	101
γ_T	2	7	5	6	6	7	3	4	6	3	6	8
ω_L	110	110	108	108	107	108	111	110	109	112	111	110
γ_L	4	7	4	5	4	4	3	4	6	3	4	5
ω_T	128	127	128	130	130	130	134	132	131	133	133	131
γ_T	3	8	8	4	4	7	2	5	13	3	4	
ω_L	130	131	130	132	132	132	136	135	133	135	135	136
γ_L	3	7	7	3	4	7	2	6	10	3	4	20
ω_T	144	144		142			142	143		147		
γ_T	11			5			8			6		
ω_L	146	145		142			145	143		147		
γ_L	11			2			8			6		
ω_T	168	167	168	164	166	164	169	170	166	170	170	165
γ_T	8	10	11	9	10	10	25	5	14	5	6	17
ω_L	184	184	183	186	186	186	189	169	190	194	194	193
γ_L	5	5	18	8	7		2	3	14	3	4	14
ω_T	193	193		198	201		196			204	202	
γ_T	10	7		6			4			4		
ω_L	196	195		210	208		197			204	202	
γ_L	10						3			5		
ω_T	210	208	208	218	222	203	213	211	205	215	214	208
γ_T	8	10	34				8	11		8	10	
ω_L	230	229	222	240	235	224	235	235	228	239	238	233
γ_L	8	10	26				4	12		6	8	
ω_T	246	248	245	247	247	244	255	252	248	255	255	251
γ_T	6	7	19				7	13	25	5	8	25
ω_L	268	268	272	264	266	272	278	276	278	279	279	278
γ_L	9	12					20			5	12	
ω_T	274	272	268	276	278	269	280	278	278	283	284	278
γ_T	8	13		20			10			5	11	
ω_L	318	317	316	350	350	318	323	322	324	334	334	332
γ_L	10	10	16			34	15	16	25	12	16	23
ω_T	356	354		364			354	355		369	368	366
γ_T	9	13					20	23		8	10	30
ω_L	364	364		374			373	373		381	381	
γ_L	15									10	12	
ω_T	368	367	356	382	385	360	374	375	358	386	385	370
γ_T			15			44	16	20	33	9		33
ω_L	466	462	457	472	474	478	468	464	467	471	471	463
γ_L	31	19	35	26	33	72	16	23	33	18	20	30

the reduced strength measured in transmission to the full strength measured in reflection suggests that the angle of misalignment for this sample was approximately 3°. The equivalent longitudinal mode was seen in transmittance at 108 cm^{-1} for CeF_3, 111 cm^{-1} for PrF_3, and 112 cm^{-1} for NdF_3.

On the basis of unpolarized emittance spectra, Rast *et al.*[30] have reported the $k\approx 0$ TO phonon frequencies for $k\|c$ (equivalent to the σ polarization) to be at 92, 100, 115, 128, 166, 192, 208, 246, 272, 353, and 368 cm^{-1} and the additional frequencies of $k\perp c$ (mixture of σ polarization and π polarization) to be at 170, 203, 235, 264, and 304 cm^{-1}. In the σ polarization, the emittance frequencies are for the most part quite close to those determined from the reflectance data. The exceptions are that neither the 92- nor the 115-cm^{-1} transitions seen in emittance are seen in either reflectance or transmittance measurements. Conversely, the emittance results show no sign of the phonon modes observed in reflectance just above and below the moderately strong band near 130 cm^{-1}. In the π polarization, the emission frequencies are not in good agreement with those observed in reflection, except for the strong lattice mode at 170 cm^{-1}. This may be due to the fact that the emittance frequencies for the π polarization were, in fact, recorded with $k\perp c$ rather than with $E\|c$ as done in reflection. As a result, the emittance experiment simultaneously excited the infrared-active modes in both orthogonal

TABLE III. Optically active phonons in proposed tysonite lattices.

Lattice space group	Formula units	Lanthanide site symmetry	Optical activity[a] IR-π	Raman-A	IR-σ	Raman-E
$P6_3/mmc$ (D_{6h}^4)	2	$\bar{6}m2$ (D_{3h})	$2A_{2u}$	$1A_{1g}$	$2E_{1u}$	$1E_{1g}$ $3E_{2g}$
$P6_3/mcm$ (D_{6h}^3)	6	mm (C_{2v})	$4A_{2u}$	$3A_{1g}$	$7E_{1u}$	$4E_{1g}$ $8E_{2g}$
$P\bar{3}c1$ (D_{3d}^4)	6	2 (C_2)	$6A_{2u}$	$5A_{1g}$	$11E_u$	$12E_g$
$P6_322$ (D_6^6)	6	2 (C_2)	$6A_2$	$5A_1$	$11E_1$	$11E_1$ $12E_2$
$P3c1$ (C_{3v}^3)	6	1 (C_1)	$11A_1$		$23E$	

[a] IR—infrared-active; π—$\mathbf{E}\|c$; σ—$\mathbf{E}\perp c$; A—nondegenerate; E—doubly degenerate.

polarizations, yielding a strongly mixed spectrum difficult to relate to the dielectric response function in either polarization.

LATTICE SPACE GROUP

Table III summarizes some results of group-theoretical vibrational analyses of several structures proposed for the tysonite lattice from x-ray–diffraction studies. From the low-temperature infrared measurements, the existence of six infrared-active modes in the π polarization ($E\|c$) and at least ten (probably eleven) infrared-active modes in the σ polarization ($E\perp c$) can be inferred. Therefore, the $P6_3/mmc$ (D_{6h}^4) lattice[12] which predicts two π and two σ infrared-active modes and the $P6_3/mcm$ (D_{6h}^3) lattice[11] which predicts four π and seven σ infrared-active modes can both be eliminated as possible tysonite lattices. The $P\bar{3}c1$ (D_{3d}^4) lattice[13–15] and the $P6_322$ (D_6^6) lattice[10] are both compatible with the infrared measurements. However, the $P6_322$ lattice can be eliminated because it predicts almost twice as many doubly degenerate Raman-active modes as observed[5] and because it predicts that all eleven of the σ infrared-active modes should also be Raman-active. Likewise, the noncentrosymmetric $P3c1$ lattice, which is consistent with the most recent x-ray studies,[13–15] can be eliminated by either infrared or Raman studies. Only the $P\bar{3}c1$ lattice seems to be consistent with both infrared and Raman measurements.

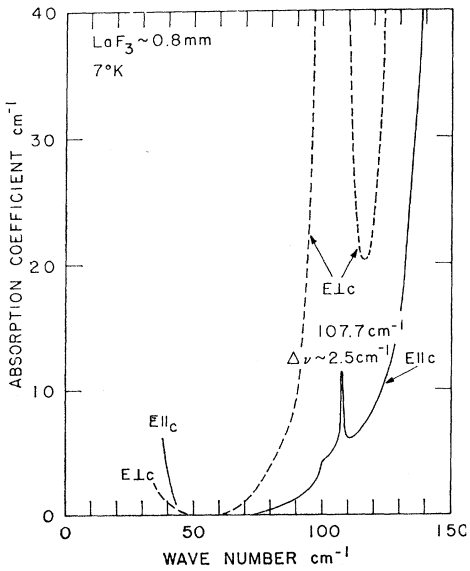

FIG. 6. Frequency dependence of the absorption coefficient of LaF_3 at 7°K calculated from transmittance data.

In addition to adequately explaining the optically active phonon spectrum, the $P\bar{3}c1$ lattice has a lanthanide ion site symmetry low enough to be compatible with all of the reported optical absorption measurements and has fluorine ion sites compatible with the spectra of H^- and D^- impurities in the lattice.[22] Those experiments in which polarized or partially polarized electronic spectra have been observed do not necessarily contradict the low site symmetry found in the $P\bar{3}c1$ lattice, since the lower site symmetry merely allows unpolarized transitions and the depolarization of a given transition may not easily be measurable.

However, the difference between the $P6_3/mcm$ and $P\bar{3}c1$ lattices is determined only by small displacements, which are of the same type as suggested by Oftedal to fully reconcile his x-ray measurements with his proposed structure,[11] and the physical properties of tysonite may be dominated by features characteristic of the approximate $P6_3/mcm$ lattice. Using the Wyckoff labels[36] for the equivalent lattice sites, the $P6_3/mcm$ lattice can be generated from the $P\bar{3}c1$ lattice by displacing the four "d" fluorines by 0.46 Å [15] so that they lie in horizontal mirror planes perpendicular to the c axis at $z=\pm\frac{1}{4}$ lattice units and by displacing the twelve "g" fluorines by 0.04 Å [15] so that they are contained within vertical mirror planes passing through the origin and the lanthanide ions. The net result of these displacements from the more symmetric $P6_3/mcm$ struc-

[36] *International Tables for X-ray Crystallography* (The Kynoch Press, Birmingham, England, 1965), Vol. I.

TABLE IV. Significant properties of the possible tysonite magnetic space groups (extracted in part from Refs. 37–40).

Magnetic space group	Magnetic crystal class	Number of magnetically distinguishable lanthanide sites	Number of independent constants[a] Pyromagnetism $H_i=a_iT$	Magneto-electric polarizability $H_i=a_{ij}E_j$	Piezomagnetism $H_i=C_{ijk}\sigma_{jk}$
$P\bar{3}c1$	$\bar{3}m$	3	0	0	2
$P\bar{3}c1'$	$\bar{3}m1'$	3	0	0	0
$P\bar{3}'c1$	$\bar{3}'m$	6	0	1	0
$P\bar{3}'c'1$	$\bar{3}'m'$	6	0	2	0
$P\bar{3}c'1$	$\bar{3}m'$	3	1	0	4
$P_c\bar{3}c1$	$\bar{3}m$	[b]	0	0	2

[a] H_i—magnetic field; a_i—pyromagnetic tensor; T—temperature; a_{ij}—magnetoelectric polarizability; E_j—electric field; C_{ijk}—piezomagnetic tensor σ_{jk}—stress tensor.
[b] See text. No proper magnetic representation for atomic sites occupied in tysonite lattice.

ture is that two B_{2u} infrared-inactive modes and the four A_{2u} infrared-active modes of the D_{6h} group combine to form the six A_{2u} infrared-active modes of the D_{3d} group. Four inactive E_{2u} modes and the seven active B_{1u} modes of D_{6h} combine to form the eleven E_u modes of D_{3d}. Therefore, the infrared spectrum associated with the $P\bar{3}c1$ lattice may be expected to consist of four π and seven σ strong reflection bands, characteristic of the $P6_3/mcm$ lattice, together with two more π and four more σ weaker reflection bands allowed only in the $P\bar{3}c1$ lattice. The experimental results confirm this and at 295°K the weaker bands observed at lower temperatures are almost completely damped out, leaving just the seven σ and four π strong infrared-active modes. This result might also be expected because the small distances that differentiate between these two lattices are comparable with typical vibrational amplitudes of ions in solids, and the increased amplitude of these vibrations as the temperature is raised would more strongly affect the weaker bands allowed only in the $P\bar{3}c1$ lattice.

MAGNETIC SPACE GROUP

In spite of the evidence given above supporting the $P\bar{3}c1$ lattice, it is not the proper tysonite structure because it predicts a magnetic ordering which is inconsistent with some of the paramagnetic and nuclear-magnetic-resonance experiments. Only three magnetically inequivalent lanthanide sites are predicted for the $P\bar{3}c1$ structure,[18] yet six magnetically inequivalent sites have been observed.[18,19]

This difficulty can be resolved by considering the 1651 Shubnikov groups[37] which include the 230 conventional space groups (Fedorov groups) as a subset. The Shubnikov groups can be generated from the Fedorov groups by assigning positive (+) or negative (−) signs (or the colors black and white) to the points of space and defining a sign (or color) inversion (anti-identity) operator associated with these signs (or colors).[38] The addition of this new operation generates 230 major (polar or single color) space groups, identical with the Fedorov groups, which contain only the new identity operator, 230 major (grey or neutral) space groups which contain both the identity and the anti-identity operator, and 1191 minor (mixed polarity or black-white) space groups which contain some complementary operators but not the anti-identity operator. Associated with these space groups are the 32 conventional (polar or single color) crystal classes, 32 (grey) crystal classes containing the anti-identity operator, and 58 minor crystal classes containing some complementary operators but not the anti-identity operator.[37–39]

For this particular application of the Shubnikov groups, the anti-identity operator defined above will be considered to be a magnetic inversion operator. A complementary operation will have the same effect as the conventional operation followed by a reversal of the local magnetic field (or equivalently, followed by a reversal of the electronic or nuclear spin generated by the conventional operator).

Table IV lists significant properties of the six magnetic space groups associated with the conventional $P\bar{3}c1$ lattice space group. Since the magnetic inversion operator does not affect physical displacement vectors or electric field vectors, any of these magnetic space groups which have the same space lattice will have the same phonon spectrum and the same optical absorption spectrum to the extent that magnetic effects can be ignored. The group $P_c\bar{3}c1$ is based upon one of the 22 new mixed-polarity lattices[37,40] rather than one of the 14 polar Bravais lattices. Since this latter group does not have a proper magnetic representation for the atomic sites occupied in the tysonite space lattice, it will not be discussed further. The other five magnetic space groups have the same space lattice as the conventional $P\bar{3}c1$

[37] N. V. Belov, N. N. Neronova, and T. S. Smirnova, Kristallografiya **2**, 315 (1957) [English transl.: Soviet Phys.—Cryst. **2**, 311 (1957)].

[38] A. M. Zamorzaev, Kristallografiya **2**, 15 (1957) [English transl.: Soviet Phys.—Cryst. **2**, 10 (1957)].

[39] S. Bhagavantam and P. V. Pantulu, Proc. Indian Acad. Sci. **59**, 1 (1964).

[40] S. Bhagavantam and P. V. Pantulu, Proc. Indian Acad. Sci. **63**, 391 (1966).

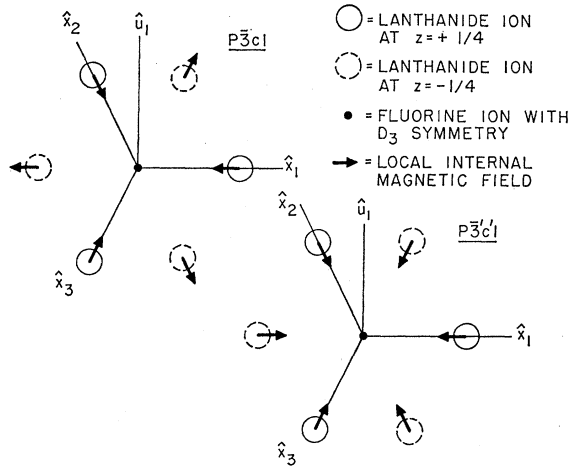

FIG. 7. Schematic illustration of the local internal magnetic fields permitted at the lanthanide ion sites in the $P\bar{3}c1$ and $P\bar{3}'c'1$ structures.

space group; therefore, they are all consistent with both the infrared and Raman studies reported above.

Due to the C_3 operator of the $\bar{3}m$ (D_{3d}) group, there will be at least three magnetically distinguishable lanthanide sites. If there are only three such sites, however, the lanthanide sites must be equivalent in pairs. Therefore, it is sufficient to determine whether any one lanthanide site is equivalent to the sites generated from it by the spatial inversion operator.

The grey magnetic space group $P\bar{3}c1'$ represents a magnetically disordered or nonmagnetic crystal. Because of the existence of the magnetic inversion operator in this group, there are no local internal magnetic fields at any point within the crystal and Kramers degeneracies are unsplit. Upon the application of an external magnetic field, any degenerate electronic states may be Zeeman split. Since the group includes the magnetic inversion operator, however, the same splitting at that site must result when the external magnetic field is reversed. Therefore, independent of the assumed spatial or magnetic parity of a magnetic tensor property associated with them, the lanthanide sites generated from each other by the spatial inversion operator must be magnetically indistinguishable.

The magnetic space groups $P\bar{3}c1$ and $P\bar{3}'c'1$ both have three ordinary C_2 operators perpendicular to the c or z axis of the crystal. If $\hat{x}$ is defined as a unit vector parallel to a C_2 axis passing through a given lanthanide site and $\hat{u}=\hat{z}\times\hat{x}$, it can be easily shown that an external field applied perpendicular to the x axis (i.e., in the u-z plane) must generate the same splitting at that site whether the field is positively or negatively directed. Therefore, just as for $P\bar{3}c1'$, the lanthanide sites generated from each other by the spatial inversion operator are indistinguishable by magnetic fields established in their common u-z plane.

It may be possible, however, to distinguish these sites from one another by the x component of the external magnetic field. Figure 7 shows the local magnetic field permitted at the lanthanide sites in these two structures. In the $P\bar{3}'c'1$ structure, the local internal magnetic fields at the two types of sites related by the spatial inversion operator are antiparallel. The external and internal magnetic fields add at one type of site and subtract at the other, resulting in a different Zeeman splitting, and allowing the sites to be magnetically distinguished. In the $P\bar{3}c1$ structure, the local internal magnetic fields at these two types of sites are parallel. As a result, the total magnetic field and the resulting Zeeman splitting at both sites are the same and the two types of sites are not magnetically distinguishable, even though the Zeeman splitting at a given site does change if the magnetic field is reversed.

By similar arguments it can be shown that $P\bar{3}c'1$ has only three magnetically distinguishable sites and is ferromagnetic, and $P\bar{3}'c1$ has six magnetically distinguishable sites and is antiferromagnetic along the z axis. Since neither of these properties has yet been observed for the tysonite lanthanide fluorides, the only magnetic space group which simultaneously explains the optically active phonon spectra and the optical absorption spectra of ions in the lattice and is consistent with the magnetic-resonance data is the $P\bar{3}'c'1$ magnetic space group.

As indicated in Table IV, either $P\bar{3}'c'1$ or $P\bar{3}'c1$ can exhibit the magnetoelectric effect ($E_i=\sum_j a_{ij}H_j$, where $\mathbf{E}\equiv$electric field, $\mathbf{H}\equiv$magnetic field, and a_{ij} is the magnetoelectric tensor). $P\bar{3}'c1$ possesses only one off-diagonal antisymmetric tensor element, $a_{xy}=-a_{yx}$. $P\bar{3}'c'1$ has two diagonal symmetric tensor elements, $a_{xx}=a_{yy}\neq a_{zz}$. A study of the symmetry of this effect, if found in the tysonite lanthanide fluorides, could confirm the proposed $P\bar{3}'c'1$ magnetic structure.

CONCLUSION

It is now possible to study in greater detail the low-energy electronic transitions of ions in a tysonite lanthanide fluoride host lattice.[34] The first-order infrared-active and the first-order Raman-active[5] phonon modes have been identified for LaF_3 through NdF_3. A magnetic space group has been proposed which is in agreement with the atomic positions predicted by x-ray–diffraction[13–15] measurements and explains the reported magnetic-resonance data.[18–20] An examination of reported near-infrared electronic transitions may now reveal some of the observed satellite lines to be vibronic transitions involving the first-order optically active phonon modes of tysonite and a study of those transitions falling in otherwise transparent spectral ranges, especially below 100 cm^{-1}, can confirm or improve current assignments of the Stark levels. With such measurements and the known crystal symmetry and phonon modes, it should be possible to determine which of the electronic transitions may be suitable for far-infrared lasers.